

Tokamak current driven by poloidally asymmetric fueling

P. Helander

Euratom/UKAEA Fusion Association, Culham Science Centre, Abingdon OX14 3DB, United Kingdom

T. Fülöp and M. Lisak

Department of Radio and Space Science, Chalmers University of Technology, 412 96 Göteborg, Sweden

(Received 13 July 2006; accepted 11 September 2006; published online 18 October 2006)

It is shown that poloidally asymmetric particle transport or fueling in a tokamak generally produces an electric current parallel to the magnetic field, in particular if the transport or fueling is up-down asymmetric. For instance, a current arises in the edge region if most particle transport across the last closed flux surface occurs in the midplane while most refueling comes from recycling near the X-point. This current is negative relative to the bulk plasma current (and thus stabilizing to peeling modes) if the ion drift is toward the X-point, and changes direction if the magnetic field is reversed. However, this current appears to be smaller than the pedestal bootstrap current under typical conditions. [DOI: 10.1063/1.2358972]

I. INTRODUCTION

The cross-field transport that takes place in a tokamak, and the refueling or heating that balances it, are in general not poloidally symmetric. Turbulent transport is usually believed to be in-out asymmetric due to the ballooning nature of the underlying instabilities, and is probably also up-down asymmetric in the edge region if the separatrix has an X-point. Similarly, the incoming particle flux that balances this transport is poloidally asymmetric, too, since much of the recycling takes place in the divertor region close to the X-point. External means of refueling, such as injection of neutral beams or pellets, is also poloidally asymmetric in general.

It was shown in a recent paper¹ that, because of toroidal effects, up-down asymmetric electron cyclotron heating of an otherwise up-down symmetric plasma produces a parallel current. Unlike other forms of current drive, this scheme does not require the waves to interact preferentially with electrons traveling in any one particular direction. On the other hand, the current drive efficiency is smaller than the usual one by a factor of the order of the collisionality ν_* , which is small in the center of the plasma.

In the present paper, we point out that a similar current can be produced by a poloidally asymmetric particle source (or sink from transport), such as that naturally occurring at the edge. As we shall see, the current arises essentially because the electrons and ions from the source, although equal in number, spread out over the flux surface in different ways. From a mathematical point of view, perhaps the easiest way to understand why the current arises is to consider the usual bootstrap current, which is obtained by solving the drift kinetic equation

$$v_{\parallel} \nabla_{\parallel} f_1 - C_e(f_1) = -\mathbf{v}_d \cdot \nabla f_0,$$

for the deviation f_1 of the electron distribution function from the Maxwellian f_0 . In a torus with large aspect ratio, the electron drift velocity \mathbf{v}_d is approximately vertical and points upward if the toroidal magnetic field is in the direction favorable for high-confinement mode (H-mode) access (and

the X-point at the bottom). Mathematically, the right-hand side of the drift kinetic equation thus represents a source above the midplane and a sink below it, if f_0 peaks in the center. In the same way, a bootstrap-like current is produced by any such source or sink, including a pure heating source such as that considered in Ref. 1 or the pure particle source considered in this paper. We calculate the magnitude of the current in the different collisionality regimes and discuss its possible practical implications. First, in Sec. II we calculate this current in the low-collisionality “banana” regime, $\nu_* \ll 1$, and provide a detailed physical picture of the mechanism producing the current. In the next section we consider the opposite regime of high collisionality and show that the dominant contribution comes from a current analogous to the Pfirsch-Schlüter current. Unlike the bootstrap-like current that arises in the banana regime, this current changes sign over the flux surface—it is partly positive and partly negative, and satisfies $\langle j_{\parallel} B \rangle = 0$, where B is the magnetic field strength, j_{\parallel} the parallel current density, and $\langle \dots \rangle$ denotes a flux-surface average. There is, however, a remnant of the bootstrap-like current with $\langle j_{\parallel} B \rangle \neq 0$ that survives at high collisionality. It is smaller than the Pfirsch-Schlüter-like current and is most easily calculated by using a Green’s function formalism, based on solving an “adjoint” kinetic equation,² as shown in Sec. IV. Our conclusions are summarized in the final section.

II. BANANA REGIME

The current is calculated from the electron drift kinetic equation averaged over turbulent fluctuations, as

$$v_{\parallel} \nabla_{\parallel} f_1 - C_e(f_1) = -\frac{e v_{\parallel} E_{\parallel}^{(A)}}{T_e} f_0 - \mathbf{v}_d \cdot \nabla f_0 + S(\mathbf{r}, v, \lambda, \sigma) + D(\mathbf{r}, v, \lambda, \sigma), \quad (1)$$

where the independent variables are the spatial coordinates \mathbf{r} , the velocity v , the normalized magnetic moment $\lambda = v_{\perp}^2 / v^2 B$, and the sign of the parallel velocity $\sigma = v_{\parallel} / |v_{\parallel}|$. C_e denotes the electron collision operator, and the terms on the

right represent various driving forces that can all produce parallel currents. Since the equation is linear and the contributions from these terms to the current are thus additive, we shall ignore the first two terms, which are conventional. The first term, containing the inductive electric field $E_{\parallel}^{(A)}$, drives the usual Ohmic current (with neoclassical corrections), and the second one produces the bootstrap current. Instead, we focus on the remaining two terms; namely, S which denotes the particle source from ionization of neutral atoms, and D , which represents the effects of anomalous transport. This term is obtained by performing an average over turbulent fluctuations and is given in Ref. 3. Since S and D appear linearly in Eq. (1), their effects on the distribution function and the current are additive, and we consider only S . The collision operator is

$$C_e(f_1) = C_e'(f_1) + \frac{m_e v_{\parallel} \nu_D^{ei}}{T_e} V_{\parallel} f_{e0},$$

$$C_e'(f_1) = C_{ee}(f_1) + \nu_D^{ei} \mathcal{L}(f_1),$$

where C_{ee} is the electron-electron collision operator, $\nu_D^{ei} = 3\pi^{1/2}/4\tau_{ei}x^3$ the ion-electron deflection frequency, with $x = v/v_{Te}$ the velocity normalized to the electron thermal speed, $v_{Te} = (2T_e/m_e)^{1/2}$, the electron-ion collision time $\tau_{ei} = 12\pi^{3/2}m_e^{1/2}T_e^{3/2}\epsilon_0^2/2^{1/2}n_iZ^2e^4 \ln \Lambda$, and the Lorentz scattering operator is defined as

$$\mathcal{L} = \frac{2v_{\parallel}}{v^2 B} \frac{\partial}{\partial \lambda} \lambda v_{\parallel} \frac{\partial}{\partial \lambda}. \quad (2)$$

If the magnetic field is up-down symmetric and the electrons are in the banana regime of low collisionality, it turns out that only the up-down asymmetric part of the source term contributes to the current to lowest order in the collision frequency. It is therefore convenient to decompose S into terms that are even and odd in the poloidal angle (measured from the midplane). If the magnetic field is up-down symmetric, we thus write $S(v, \lambda, \psi, \theta) = S_+(v, \lambda, \psi, \theta) + S_-(v, \lambda, \psi, \theta)$, with

$$S_{\pm}(v, \lambda, \psi, \theta) = \frac{1}{2}[S(v, \lambda, \psi, \theta) \pm S(v, \lambda, \psi, -\theta)]. \quad (3)$$

Here and in the following, we take the range of the poloidal angle to be $-\pi < \theta \leq \pi$. Since the orbit average of the odd part vanishes, $\int S_- dt = 0$ when taken over a period of any particle orbit, it can be expressed as $S_- = v_{\parallel} \nabla_{\parallel} h$ for some function $h(v, \lambda, \psi, \theta)$. If, for simplicity, the fueling is isotropic in velocity space and localized at a single poloidal angle, i.e., $\theta = \theta_*$, the particle source can be represented by

$$S(v, \lambda, \psi, \theta) = S_0(v, \lambda, \psi) \delta(\theta - \theta_*), \quad (4)$$

and then h may be chosen as

$$h = \frac{qR_* S_0(v, \lambda, \psi) H(\theta)}{2\sigma v \sqrt{1 - \lambda B_*}}, \quad (5)$$

with $B_* = B(\theta_*) = B(-\theta_*)$, $qR_* = 1/\nabla_{\parallel} \theta|_{\theta=\theta_*}$, and

$$H(\theta) = \begin{cases} -\text{sign } \theta_*, & |\theta| < |\theta_*|, \\ 0, & |\theta_*| < |\theta|. \end{cases} \quad (6)$$

A source that is distributed over a range of poloidal angles can be represented in the obvious way by a linear combination (integral) of such functions h .

If the magnetic field is not up-down symmetric, it is convenient to use a poloidal angle θ with the property that $\nabla_{\parallel} \theta$ is constant on each flux surface. This is accomplished by defining θ through the relation

$$\frac{d\theta}{d\vartheta} = \frac{2\pi}{\nabla_{\parallel} \vartheta} \bigg/ \int_{-\pi}^{\pi} \frac{d\vartheta}{\nabla_{\parallel} \vartheta}, \quad (7)$$

where ϑ is the usual poloidal angle. The latter may, in fact, be defined arbitrarily (as long as it is 2π -periodic) since Eq. (7) is independent of the definition of ϑ . Within this definition of θ , the origin $\theta=0$ can be chosen arbitrarily. If the source is given by Eq. (4), it is convenient to choose the origin such that $B(-\theta_*) = B(\theta_*)$. With this choice of θ , we still have

$$S_-(\theta) = \frac{1}{2}[S(\theta) - S(-\theta)] = v_{\parallel} \nabla_{\parallel} h, \quad (8)$$

with h given by Eqs. (5) and (6).

The kinetic equation can now be written as

$$v_{\parallel} \nabla_{\parallel} (f_1 - h) = C_e'(f_1) + \frac{m_e v_{\parallel} \nu_D^{ei}}{T_e} V_{\parallel} f_{e0} \quad (9)$$

and can be solved by the usual techniques of neoclassical transport theory.^{4,5} There are two driving terms in Eq. (9), originating from the source S (appearing through the function h) and the ion flow V_{\parallel} , respectively, and we may decompose the solution accordingly:

$$f_1 = f_S + f_V. \quad (10)$$

The term f_V , which is driven by V_{\parallel} , is well known from the theory of neutral-beam current drive, where it represents the electron ‘‘shielding’’ of the beam current and has been calculated many times in the literature.⁶ We therefore restrict our attention to the source-driven part of the electron distribution function, which satisfies Eq. (9) without the last term on the right. In the banana regime of small collisionality, $g = f_S - h$ is independent of the poloidal angle in lowest order, $\nabla_{\parallel} g = 0$. From the next-order equation, it follows that g vanishes in the trapped region and satisfies

$$\left\langle \frac{B}{v_{\parallel}} C_e'(g + h) \right\rangle = 0 \quad (11)$$

in the passing region, where angular brackets denote the flux-surface average:

$$\langle \cdots \rangle = \int_{-\pi}^{\pi} (\cdots) \frac{d\theta}{B} \bigg/ \int_{-\pi}^{\pi} \frac{d\theta}{B}. \quad (12)$$

We expect most of the particles in f_S to have kinetic energies much smaller than T_e . Indeed, the calculation in the Appendix shows that when S describes an ionization source the spectrum of the emitted electrons is mainly localized to energies comparable to the ionization energy, which is usually

far lower than the electron temperature in the plasma edge region. Since the frequency of electron-ion collisions scales as v^{-3} and that of electron-electron collisions as v^{-2} for small v , the latter can be neglected, and the solution of Eq. (11) becomes

$$\langle v_{\parallel} \rangle \frac{\partial g}{\partial \lambda} = - \left\langle v_{\parallel} \frac{\partial h}{\partial \lambda} \right\rangle. \quad (13)$$

The current associated with g is

$$j_{\parallel}^g = -e \int v_{\parallel} g d^3v = -\frac{neqR_*B}{2B_*} J(\theta_*), \quad (14)$$

where, for simplicity, we have taken the source to be isotropic and written

$$\dot{n}(\psi) = \int S_0(v, \psi) d^3v \quad (15)$$

and

$$J(\theta_*) = \frac{B_*^2}{4} \int_0^{\lambda_c} \frac{\langle H(\theta) \sqrt{1-\lambda B} \rangle}{\langle \sqrt{1-\lambda B} \rangle} \frac{\lambda d\lambda}{(1-\lambda B_*)^{3/2}}. \quad (16)$$

In the usual limit of a circular flux surface with large aspect ratio, $B \approx B_0(1 - \epsilon \cos \theta)$, the flux-surface averages can be calculated analytically to lowest order in $\epsilon^{1/2}$. In the passing region of velocity space

$$\langle H(\theta) \sqrt{1-\lambda B} \rangle = \sqrt{\frac{2\epsilon}{2\epsilon + k^2}} \frac{2E(\theta_*/2, k)}{\pi} \text{sign } \theta_*, \quad (17)$$

where E denotes an incomplete elliptic integral and

$$k^2 = \frac{2\epsilon \lambda B_0}{1 - \lambda B_0(1 - \epsilon)}. \quad (18)$$

Hence, the expansion of $J(\theta_*)$ in the small parameter $\epsilon^{1/2}$ is

$$J(\theta_*) = -\frac{\text{sign } \theta_*}{\sqrt{\epsilon}} \int_0^1 \frac{E(\theta_*/2, k) dk}{[2 - (1 - \cos \theta_*)k^2]^{3/2} E(\pi/2, k)} + O(1) \quad (19)$$

and the current (14) becomes

$$j_{\parallel}^g \approx -\frac{neqRJ(\theta_*)}{2}. \quad (20)$$

Since this expression contains the factor $J(\theta_*)$, which is of order $\epsilon^{1/2}$, the current carried by g is $O(\epsilon^{-1/2})$ larger than that carried by h , which is obtained by taking the appropriate integral of Eq. (5) and contains no such large factor. The total current is thus, finally,

$$j_{\parallel} = neV_{\text{th}} - e \int v_{\parallel} (f_V + g + h) d^3v \approx j_{\parallel}^g, \quad (21)$$

since the current associated with f_V approximately cancels the ion current. In the next subsection, we calculate corrections to this result due to electron-electron collisions.

In order to clarify the direction of the current, we express the magnetic field in the standard form $\mathbf{B} = I(\psi) \nabla \varphi + \nabla \varphi \times \nabla \psi$ and choose the toroidal angle φ to be in the di-

rection of the main plasma current, so that $\nabla \psi$ points radially outward from the magnetic axis. The drift velocity is either outward or inward depending on the sign of

$$(\mathbf{B} \times \nabla B) \cdot \nabla \psi = -I\mathbf{B} \cdot \nabla B = -\frac{\epsilon I B^2}{qR} \sin \theta, \quad (22)$$

where we have taken $B = B_0(1 - \epsilon \cos \theta)$ and used $\nabla_{\parallel} \theta = 1/qR$. The φ component of the source-driven current is

$$j_{\varphi} \approx \frac{I j_{\parallel}}{RB} = -\frac{neqIJ(\theta_*)}{2B} = \frac{\epsilon neI^2 B}{2R(\mathbf{B} \times \nabla B) \cdot \nabla \psi} \Big|_{\theta=\theta_*} J(\theta_*) \sin \theta_*, \quad (23)$$

where $J(\theta_*) \sin \theta_*$ is negative [see Eq. (19)]. The source-driven current is thus in the same direction as the main plasma current if the ion grad- B drift is inward, $(\mathbf{B} \times \nabla B) \cdot \nabla \psi < 0$, at the location of the source, and in the opposite direction otherwise. Specifically, if the magnetic configuration is favorable for H-mode access (ion drift toward the single X-point) and the fueling occurs at the X-point, then the source-driven current is opposite to the main plasma current.

A. The effect of electron-electron collisions

It is customary in neoclassical theory to model the electron-electron collision operator by

$$C_m^{ee}(g) = \nu_D^{ee} \left[\mathcal{L}(g) + \frac{m v_{\parallel}}{T_e} u \right] f_{e0}, \quad (24)$$

where u is a coefficient that is chosen so as to ensure momentum conservation.⁷ In more accurate calculations of transport, u is sometimes allowed to vary with velocity in a simple way, usually by $u = u_0 + u_1 x^2$. (For instance, this is effectively what is done in the Hirshman-Sigmar moment formalism.⁸) For the purpose of the present paper, however, this approximation is not good enough if the typical energy of electrons from the source is much lower than the bulk electron temperature. Instead, we shall let u depend on energy in such a way that the $P_1(\xi)$ -moment of the full (linearized) collision operator is exactly reproduced by the model operator (24). Here $\xi = v_{\parallel}/v$, $P_1(\xi) = \xi$ denotes a Legendre polynomial, and a superscript ⁽¹⁾ will be used for the P_1 component of any function of velocity space; e.g.,

$$g^{(1)}(v) = \frac{3}{2} \int_{-1}^1 g(v, \xi) \xi d\xi. \quad (25)$$

This moment of the model operator is

$$C_m^{(1)}(g) = \nu_D^{ee} \left(-g^{(1)} + \frac{m_e v}{T_e} u f_{e0} \right) \quad (26)$$

while that of the full linearized operator is equal to⁵

$$C_{ee}^{(1)}(g) = -\nu_D^{ee} g^{(1)} + \frac{1}{2v^2} \frac{\partial}{\partial v} \left[v^3 \nu_s \left(g^{(1)} + \frac{T_e}{m_e v} \frac{\partial g^{(1)}}{\partial v} \right) \right] + \frac{e^4 \ln \Lambda}{m_e^2 \epsilon_0^2} \left[g^{(1)} + \frac{m_e}{T_e} \varphi^{(1)} - \left(\frac{m_e v}{T_e} \right)^2 \frac{\partial^2 \psi^{(1)}}{\partial v^2} \right] f_{e0}. \quad (27)$$

Here

$$\frac{1}{v^2} \frac{\partial}{\partial v} \left(v^2 \frac{\partial \varphi^{(1)}}{\partial v} \right) = g^{(1)}, \quad (28)$$

$$\frac{1}{v^2} \frac{\partial}{\partial v} \left(v^2 \frac{\partial \psi^{(1)}}{\partial v} \right) = \varphi^{(1)} \quad (29)$$

are Rosenbluth potentials, $\nu_s = 4\hat{\nu}_{ee} G(v/v_{Te})/(v/v_{Te})$ is the slowing-down frequency, $G(x) = [\text{erf}(x) - x \text{erf}'(x)]/2x^2$ the Chandrasekhar function, and $\hat{\nu}_{ee} = n_e e^4 \ln \Lambda / 4\pi \epsilon_0^2 m_e^2 v_{Te}^3$. For subthermal velocities, $v \ll v_{Te}$, we have

$$\left(\frac{m_e v}{T_e} \right)^2 \frac{\partial^2 \psi^{(1)}}{\partial v^2} \ll \frac{m_e}{T_e} \varphi^{(1)} \ll g^{(1)} \ll \frac{T_e}{m_e v} \frac{\partial g^{(1)}}{\partial v}, \quad (30)$$

$\nu_s \approx 8\hat{\nu}_{ee}/3\pi^{1/2}$, and

$$\frac{1}{2v^2} \frac{\partial}{\partial v} \left(v^3 \nu_s \frac{T_e}{m_e v} \frac{\partial g^{(1)}}{\partial v} \right) \gg \frac{e^4 \ln \Lambda}{m_e^2 \epsilon_0^2} g^{(1)} f_{e0}. \quad (31)$$

This means that energy diffusion dominates in the full linearized collision operator, and equating (26) with (27) gives

$$\frac{m_e v}{T_e} u f_{e0} = \frac{1}{2} \frac{\partial}{\partial v} \left(v^2 \frac{\partial g^{(1)}}{\partial v} \right). \quad (32)$$

Equation (11) now becomes

$$\langle v_{\parallel} \rangle \frac{\partial g}{\partial \lambda} = - \left\langle v_{\parallel} \frac{\partial h}{\partial \lambda} \right\rangle - \frac{m_e v^2}{2T_e} \frac{\nu_D^{ee}}{\nu_D^{ee} + \nu_D^{ei}} \langle uB \rangle f_{e0}, \quad (33)$$

so that $f_S^{(1)} = g^{(1)} + h^{(1)}$ is given by

$$f_S^{(1)} = \frac{3qR_* S_0(v)B}{2vB_*} \left[J(\theta_*) + H(\theta) \left(1 - \sqrt{1 - \frac{B_*}{B}} \right) \right] + \frac{m_e v B f_c}{\langle B^2 \rangle T_e} \frac{\nu_D^{ee}}{\nu_D^{ee} + \nu_D^{ei}} \langle uB \rangle f_{e0}, \quad (34)$$

where $\nu_D^{ei} = (4\hat{\nu}_{ei}/3\sqrt{\pi}x^3) \approx \nu_D^{ee}/x$ and

$$f_c = \frac{3\langle B^2 \rangle}{4} \int_0^{1/B_{\max}} \frac{\lambda d\lambda}{\langle \sqrt{1 - \lambda B} \rangle} \quad (35)$$

is the effective fraction of circulating particles.⁸ In the limit of large aspect ratio and circular flux surfaces, this quantity becomes $f_c \approx 1 - 1.46\sqrt{\epsilon}$. Using $g^{(1)}$ from (34), Eq. (32) gives

$$u f_{e0} = \frac{1}{2} \frac{\partial}{\partial v} v^2 \frac{\partial}{\partial v} \left\{ \frac{3qR_* T_e S_0(v)B}{2vB_* m_e} \left[J(\theta_*) + H(\theta) \right] \times \left(1 - \sqrt{1 - \frac{B_*}{B}} \right) + \frac{f_c B v^2}{v_{Te} \langle B^2 \rangle} \langle Bu \rangle f_{e0} \right\}, \quad (36)$$

where the last term can be neglected, being $O(v_s/v_{Te})$ smaller than the left-hand side, where v_s is the characteristic velocity of the source particles. This term is therefore of

order $(v_s/v_{Te})^2$ smaller than the leading order terms in g . The current associated with g thus becomes approximately equal to

$$j_{\parallel}^g = -e \int v_{\parallel} g d^3v \approx -\frac{eqR_* B}{2B_*} \left[\dot{n} J(\theta_*) + \frac{10f_c}{v_{Te}} \left\langle J(\theta_*) + \frac{H(\theta)B^2}{\langle B^2 \rangle} \right\rangle \times \left(1 - \sqrt{1 - \frac{B_*}{B}} \right) \right] \int S_0(v) 4\pi v^3 dv, \quad (37)$$

where the first term is identical to the result (14) found in the Lorentz limit, and the second term represents the correction due to electron-electron collisions. This correction is formally small, of order v_s/v_{Te} , but has a fairly large coefficient and may therefore be important in practice. In the limit of large aspect ratio, the current becomes

$$j_{\parallel} \approx -\frac{eqRJ(\theta_*)}{2} \left[\dot{n} + \frac{10}{v_{Te}} \int S_0(v) 4\pi v^3 dv \right]. \quad (38)$$

B. Physical picture

The physical origin of the current can be understood by considering the fate of electrons added to the plasma in a single point, which we take to be somewhere below the midplane, $-\pi < \theta_* < 0$. In addition, it is useful to assume initially that the source is not isotropic in velocity space but instead such that the particles have no parallel velocity at birth. This implies that all particles are born on trapped orbits at the lower bounce point, and immediately after birth start moving toward the upper bounce point. Each particle gets accelerated in the parallel direction by the mirror force, and by the time it reaches the midplane it has acquired a parallel velocity of order

$$v_{\parallel} \sim v \epsilon^{1/2}.$$

If electrons are continuously added to the plasma in this way, at a rate \dot{n}_{tr} per unit time and volume, there will thus be more co-moving trapped electrons than counter-moving ones (if the direction of the magnetic field is such that particles have $v_{\parallel} > 0$ when traveling upward); see Fig. 1. The ratio of the number of co- to counter-moving trapped electrons is

$$\frac{n_{\text{co}}}{n_{\text{counter}}} \Big|_{\text{trapped}} \sim \frac{\dot{n}_{\text{tr}} qR/v_{\parallel}}{n_{\text{tr}}} \sim \frac{\dot{n}_{\text{tr}} qR}{v n \epsilon}, \quad (39)$$

where $n_{\text{tr}} \sim \epsilon^{1/2}$ is the trapped-electron density and qR/v_{\parallel} the time it takes a trapped electron to travel from the lower to the upper bounce point.

So far we have only considered collisionless particles. However, particles with different v_{\parallel}/v interact through pitch-angle scattering collisions and this has implications for the net current. If the trapped and circulating populations are to be in a collisional equilibrium with each other, there must be a surplus of co-passing particles similar to that of co-trapped ones; i.e.,

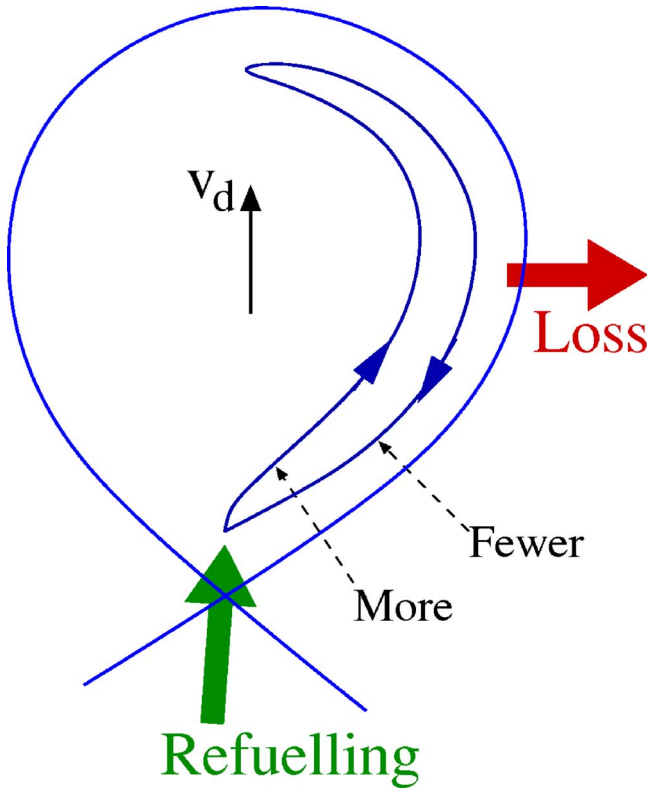


FIG. 1. (Color online) An up-down asymmetric particle source/sink causes there to be more co-trapped than counter-trapped particles, or vice versa.

$$\frac{n_{\text{co}}}{n_{\text{counter}}} \Big|_{\text{circulating}} \sim \frac{\dot{n}_{\text{tr}} q R}{v n \epsilon}.$$

Not being subject to magnetic trapping, the circulating population is free to adjust its mean parallel speed to satisfy this condition. This results in a parallel current density of order

$$j_{\parallel} \sim -e v (n_{\text{co}} - n_{\text{counter}}) \sim -\frac{\dot{n}_{\text{tr}} e q R}{\epsilon}. \quad (40)$$

Finally, if the source is instead isotropic in velocity space but still localized to a single point below the midplane, the number of particles born on trapped orbits will be $\dot{n}_{\text{tr}} \sim \dot{n} \epsilon^{1/2}$, where \dot{n} is the total source rate. These trapped particles have bounce points at $\pm \theta_b$ with $|\theta_b| > |\theta_*|$, and the ones born with negative parallel velocity ($\dot{\theta} < 0$) will reach their lower bounce point, $-\theta_b$, before their upper one, while those born with positive v_{\parallel} will first bounce above the midplane. Electrons with negative v_{\parallel} therefore reverse their velocity sooner than those with positive v_{\parallel} , which implies that a short time (of the order of half the bounce time) after birth, most particles will have $v_{\parallel} > 0$. (This is particularly clear in the extreme case of fueling just below the inner midplane, $\theta_* = -\pi + \delta$, $\delta \rightarrow 0+$, where the source only adds co-moving particles to the plasma.) This implies that a surplus of co-trapped particles of order (39) arises, and a current similar to Eq. (40) is again produced; i.e.,

$$j_{\parallel} \sim -\frac{\dot{n} e q R}{2 \epsilon^{1/2}}. \quad (41)$$

It is seen from this physical picture that the mechanism producing the fueling-driven current is rather similar to that of the bootstrap current, where the difference in co- and counter-moving trapped electrons is instead created by the radial density and temperature gradients.

III. PFIRSCH-SCHLÜTER-LIKE CURRENT

If a poloidally varying particle source is present in a collisional plasma, it causes a parallel current analogous to the usual Pfirsch-Schlüter current. This current can be calculated from fluid equations obtained by taking moments of Eq. (1). Neglecting the cross-field drift (which gives rise to the usual Pfirsch-Schlüter current), we obtain the steady-state continuity equation

$$B \nabla_{\parallel} \left(\frac{n_e V_{e\parallel}}{B} \right) = s_p(\theta), \quad (42)$$

where the right-hand side represents the particle source

$$s_p(\theta) = \int (S + D) d^3 v. \quad (43)$$

This must vanish on a flux-surface average, $\langle s_p \rangle = 0$, so that the source is balanced by transport in steady state. It follows that the parallel particle flux is

$$n_e V_{e\parallel} = B \int_0^{\theta} \frac{s_p(\theta') d\theta'}{B \nabla_{\parallel} \theta'} + K(\psi), \quad (44)$$

where the integration constant $K(\psi)$ is a flux function.

The physical reason that the Pfirsch-Schlüter-like current appears is that the poloidal variation of the source causes the electron pressure, the electron temperature, and the electrostatic potential to acquire a poloidal variation, e.g., $p_e = \bar{p}_e(\psi) + \tilde{p}_e(\psi, \theta)$, where $\tilde{p}_e \ll \bar{p}_e$ if the source is weak. The accompanying parallel gradients drive a flow of the electron fluid relative to the ion fluid, i.e., a current, in accordance with the parallel Ohm's law

$$V_{e\parallel} - V_{i\parallel} = -l_{11} \left(\frac{\nabla_{\parallel} \tilde{p}_e}{\bar{p}_e} - \frac{e \nabla_{\parallel} \phi}{\bar{T}_e} \right) - l_{12} \frac{\nabla_{\parallel} \tilde{T}_e}{\bar{T}_e}. \quad (45)$$

The transport coefficients l_{jk} depend on the composition of the plasma and have been calculated by numerous authors, including Spitzer and Härm⁹ and Braginskii¹⁰ who considered a pure plasma without impurities. We do not need these coefficients, but merely the fact that the flux-surface average of Eq. (45) multiplied by B gives

$$\langle j_{\parallel} B \rangle = 0. \quad (46)$$

This property is characteristic of the Pfirsch-Schlüter current, and implies that the current changes sign over the flux surface. Note that there may well be a net toroidal current although $\langle j_{\parallel} B \rangle = 0$. Combining this result with Eq. (44) gives the local current density

$$\frac{j_{\parallel}}{B} = n_e e \left(\frac{V_{\parallel}}{B} - \frac{\langle V_{\parallel} B \rangle}{\langle B^2 \rangle} \right) - e \int_0^{\theta} \frac{s_p(\theta') d\theta'}{B \nabla_{\parallel} \theta'} + \frac{e}{\langle B^2 \rangle} \left\langle B^2 \int_0^{\theta} \frac{s_p(\theta') d\theta'}{B \nabla_{\parallel} \theta'} \right\rangle. \quad (47)$$

In a tokamak with large aspect ratio, this current is $O(\epsilon^{1/2})$ smaller than the bootstrap-like current derived in Sec. II.

IV. BOOTSTRAP-LIKE CURRENT AT HIGH COLLISIONALITY

Although the Pfirsch-Schlüter-like current calculated in the previous section dominates, the current still has a finite component with $\langle j_{\parallel} B \rangle \neq 0$. In order to calculate this bootstrap-like current, both in the Pfirsch-Schlüter, high-collisionality regime and in the plateau regime of intermediate collisionality, $1 \ll \nu_* \ll \epsilon^{-3/2}$, it is more convenient to employ an “adjoint” (Green’s function) formalism² than to solve the kinetic equation

$$v_{\parallel} \nabla_{\parallel} f_S - C'_e(f_S) = S. \quad (48)$$

A. Adjoint technique

The adjoint equation is

$$v_{\parallel} \nabla_{\parallel} G + C'_e(G) = v_{\parallel} B f_0 / \langle B^2 \rangle. \quad (49)$$

Multiplying this equation by f_S/f_0 , integrating over velocity space, and taking the flux-surface average gives

$$\left\langle \int \frac{f_S}{f_0} \left[v_{\parallel} \nabla_{\parallel} G + C'_e(G) - \frac{v_{\parallel} B f_0}{\langle B^2 \rangle} \right] d^3 v \right\rangle = 0, \quad (50)$$

and from Eq. (48) follows similarly

$$\left\langle \int \frac{G}{f_0} [v_{\parallel} \nabla_{\parallel} f_S - C'_e(f_S) - S] d^3 v \right\rangle = 0. \quad (51)$$

Adding these two equations and using the self-adjointness of C'_e gives the electron current as

$$\frac{\langle j_{\parallel} B \rangle}{\langle B^2 \rangle} = - \frac{e}{\langle B^2 \rangle} \int v_{\parallel} f_S d^3 v = e \left\langle \int \frac{G S}{f_0} d^3 v \right\rangle. \quad (52)$$

Thus, the solution to the adjoint equation (49) enables the average $\langle j_{\parallel} B \rangle$ of the current to be calculated in a straightforward way. In order to obtain this solution, we first write it as

$$G = - \frac{v_{\parallel} f_{\text{sp}}(v) B}{\langle B^2 \rangle} + k, \quad (53)$$

where f_{sp} is the Spitzer function, satisfying

$$C'_e(v_{\parallel} f_{\text{sp}}) = -v_{\parallel} f_0. \quad (54)$$

The equation for k then becomes

$$v_{\parallel} \nabla_{\parallel} k + C'_e(k) = v^2 f_{\text{sp}}(v) P_2(\xi) \nabla_{\parallel} B / \langle B^2 \rangle, \quad (55)$$

with $P_2(\xi) = (3\xi^2 - 1)/2$, and this equation will be considered in the plateau and Pfirsch-Schlüter regimes separately.

B. Plateau regime

In the plateau regime of intermediate collisionality, $\epsilon \ll 1 \ll \nu_* \ll \epsilon^{-3/2}$,

$$\nabla_{\parallel} B \simeq \frac{\epsilon B \sin \theta}{qR}, \quad (56)$$

on circular flux surfaces, and Eq. (55) becomes

$$\frac{v_{\parallel}}{qR} \frac{\partial k}{\partial \theta} - C'_e(k) = \frac{\epsilon v^2 f_{\text{sp}}(v)}{qRB} P_2(\xi) \sin \theta. \quad (57)$$

For $|\xi| \ll 1$, this equation reduces to

$$\xi \frac{\partial k}{\partial \theta} + \frac{qR(v_D^{ee} + v_D^{ei})}{2v} \frac{\partial^2 k}{\partial \xi^2} = - \frac{\epsilon v f_{\text{sp}}(v)}{2B} \sin \theta, \quad (58)$$

and has the solution^{4,5}

$$k = \frac{N \epsilon v f_{\text{sp}}}{2B} \int_0^{\infty} e^{-x^3/3} \sin(\theta + x/N) dx, \quad (59)$$

where $N = [2v/(v_D^{ee} + v_D^{ei}) qR]^{1/3} \gg 1$. Only the part of k that is even in ξ contributes to the current (52), and this part becomes

$$k_{\text{even}} = \frac{\pi \epsilon v f_{\text{sp}}}{2B} \delta(\xi) \sin \theta, \quad (60)$$

in the limit $N \rightarrow \infty$. The current (49) is thus

$$\langle j_{\parallel} B \rangle = \frac{\pi \epsilon e B}{4} \int \frac{v f_{\text{sp}}}{f_{e0}} \delta(\xi) \langle S(v, \xi) \sin \theta \rangle d^3 v, \quad (61)$$

and is a factor of order $1/\nu_*$ smaller than that found in the banana regime.

C. Pfirsch-Schlüter regime

In the Pfirsch-Schlüter regime of high collisionality, $\langle j_{\parallel} B \rangle$ becomes very small, just like the ordinary bootstrap current. Equation (55) is to lowest order approximated by

$$C'_e(k) = v^2 f_{\text{sp}}(v) P_2(\xi) \nabla_{\parallel} B / \langle B^2 \rangle, \quad (62)$$

and has the approximate solution

$$k \simeq \frac{v^2 f_{\text{sp}}(v) \nabla_{\parallel} B}{\nu_T(v) \langle B^2 \rangle} P_2(\xi), \quad (63)$$

where $\nu_T = (2 - T_e/m_e v^2) \nu_s - \nu_D^{ee} - \nu_D^{ei}$ is the relaxation frequency for perturbations with $P_2(\xi)$ dependence on pitch angle.⁸ (To arrive at this approximate result, one takes the liberty of replacing the collision operator by a Krook operator with the collision frequency ν_T .) The current (52) thus becomes a factor ν_*^{-2} smaller than the corresponding current in the banana regime or the Pfirsch-Schlüter-like current calculated in Sec. III. If the pitch-angle dependence of the source has no $P_2(\xi)$ component, the integral (52) vanishes in lowest order, and the current becomes even smaller.

V. CONCLUSIONS

We have established that a poloidally asymmetric particle source, or poloidally asymmetric transport, generally causes a current to flow along the magnetic field. The only

exception occurs if the source or transport is up-down symmetric in the sense that it is equal at those points of each flux surface where the magnetic field strength B is equal. (This is, e.g., the case for the emission of synchrotron radiation, which would otherwise drive a plasma current.) The current is caused by toroidal effects, and is similar in character to the bootstrap current when the collisionality is low and to the Pfirsch-Schlüter currents when the collisionality is high. In the former case, the current density is of order

$$j_{\parallel} \sim -\frac{\dot{n}eqR}{2\epsilon^{1/2}}, \quad (64)$$

where \dot{n} is the source strength (number of particles added in unit time and volume), and at high collisionality the current is a factor $\epsilon^{1/2}$ smaller. The current (64) is calculated by solving the electron drift kinetic equation. There is also an analogous ion current, which is, however, largely shielded by the electrons (if ϵ is small) but does cause plasma rotation, as discussed at the end of this section.

The direction of the current (64) depends on the poloidal location of the source/sink and on the direction of the magnetic field and plasma current. The fueling-driven current is in the opposite direction to the main plasma current if ion grad-B drift is outward at the location of the source. This is, for instance, the case for a single-null divertor configuration with the field in the direction favorable for H-mode access. If most of the recycling takes place near the X-point, the fueling-driven current is thus stabilizing to peeling modes, and it is tempting to speculate that this is what facilitates access to H-mode. However, it appears that the fueling current is smaller than the bootstrap current under typical H-mode conditions. The bootstrap current density is

$$j_{\text{bs}} \sim -\frac{2\epsilon^{1/2} dp_e}{B_{\theta} dr}, \quad (65)$$

where p_e is the electron pressure, so the total pedestal bootstrap current is

$$I_{\text{bs}} \sim \frac{4\pi a \epsilon^{1/2} p_{\text{ped}}}{B_{\theta}}, \quad (66)$$

where a is the minor radius of the plasma column and p_{ped} the pedestal pressure. The latter is typically of order 10^4 Pa in DIII-D and JET. The total fueling current obtained by integrating (64) over the poloidal cross section of the torus is

$$I_f \sim -\frac{\dot{N}eq}{4\pi\epsilon^{1/2}}, \quad (67)$$

where \dot{N} is the total number of particles supplied by the source in unit time (the volume integral of \dot{n}). The ratio of fueling current to bootstrap current is thus

$$\frac{I_f}{I_{\text{bs}}} \sim -\frac{\dot{N}eB}{16\pi^2 a p_{\text{ped}}}. \quad (68)$$

The main difficulty in applying this estimate lies in the uncertainty of \dot{N} . In principle, this quantity is measured through the D_{α} photon count, from which the total in-vessel ionization events can be determined. However, most of these typically occur in the divertor region, and it is only ionization inside the separatrix that contributes to the current. A rough estimate for \dot{N} can be obtained from the gas puffing rate, giving typically $\dot{N}e \sim 1\text{--}10$ kA in JET. Alternatively, it can be deduced from edge modeling, where $\dot{N}e \sim 2$ kA was found in DIII-D¹¹ in a plasma with $p_{\text{ped}} \approx 6.5$ kPa. In either case, the ratio (68) becomes quite small. These very approximate estimates suggest that the fueling current is relatively small in typical H-mode plasmas, but do not necessarily mean that it is always unimportant. The fueling current may, for instance, have a radial profile that makes it affect edge magnetohydrodynamic stability.

We close by commenting on the issue of edge plasma rotation. It has been observed in Alcator C-Mod that this rotation depends strongly on the location of the X-point and has intriguing links to the low- to high-confinement mode (L-H) transition.¹² The mechanism attributed to the cause of the rotation is that the transport mostly occurs in the outer midplane, from where plasma flows to the divertor along open lines in the scrape-off layer. Depending on whether the X-point is at the top or at the bottom, most of this flow is either in the co-current or in the counter-current direction. It is believed that these scrape-off layer flows cause the plasma inside the separatrix to rotate accordingly, presumably through cross-field viscosity. However, the results of the present paper suggest another explanation. If the calculation done here for the electrons is instead carried out for the ion species, one arrives at the conclusion that up-down asymmetric fueling creates plasma rotation, which in turn drives radial impurity transport.¹³ This rotation is comparable to that caused by parallel plasma flows in the scrape-off layer, and it thus seems likely that the two mechanisms should operate in parallel.

ACKNOWLEDGMENTS

This work was funded jointly by the United Kingdom Engineering and Physical Sciences Research Council and by the European Communities under Association Contracts between EURATOM, UKAEA, and *Vetenskapsrådet*. The views and opinions expressed herein do not necessarily reflect those of the European Commission.

APPENDIX: EJECTED ELECTRON DISTRIBUTION FOR ELECTRON-IMPACT IONIZATION OF ATOMIC HYDROGEN

The cross section for the ionization of a hydrogen atom with the emission of a secondary electron in a given direction is given in Refs. 14–16 under the assumption that the energy of the secondary electron is small in comparison with that of the primary (Born approximation). The differential cross section for production of a secondary electron with a given wave vector κ is

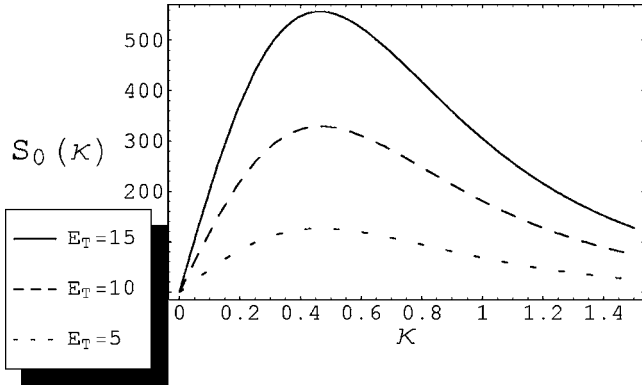


FIG. 2. Energy spectrum of an ionization source: S_0/C as a function of κ (wave vector normalized to the Bohr radius) for different energies E_T .

$$d\sigma = \frac{2^{10} k' \kappa}{k q^2} \frac{[q^2 + (1 + \kappa^2)/3] e^{-(2/\kappa) \tan^{-1}[2\kappa/(q^2 - \kappa^2 + 1)]}}{[(q + \kappa)^2 + 1]^3 [(q - \kappa)^2 + 1]^3 (1 - e^{-2\pi/\kappa})} d\omega d\kappa, \quad (\text{A1})$$

where \mathbf{k} and \mathbf{k}' are the wave vectors of the incident electron before and after the collision, respectively, and $\mathbf{q} = \mathbf{k} - \mathbf{k}'$. All wave vectors are normalized to the inverse Bohr radius $a_0 = (4\pi\epsilon_0\hbar^2/me^2)$, and the energies are normalized to the Rydberg energy $\text{Ry} = me^4/2\hbar^2(4\pi\epsilon_0)^2 = 13.6$ eV, so that $E = k^2$. Since $q^2 = k^2 + k'^2 - 2kk' \cos \theta$, for given k and k' we have $q dq = kk' \sin \theta d\theta = kk' do / (2\pi)$, where do is an element of solid angle about the direction of the scattered electron. In an ionizing collision, the energy transfer should be equal to the sum of the threshold for ionization and the energy of the secondary electron: $k^2 - k'^2 = 1 + \kappa^2$. The minimum and maximum q are $q_{\min} = k - k'$ and $q_{\max} = k + k'$, and for large incident energies $q_{\min} = (1 + \kappa^2)/(2k)$ and $q_{\max} = 2k$, to a first approximation. Numerical integration with $do = 2\pi q dq / (kk')$ gives the differential cross section $d\sigma/d\kappa$:

$$\frac{d\sigma}{d\kappa} = \frac{2^{11} \pi \kappa}{k^2 (1 - e^{-2\pi/\kappa})} \times \int_{(1+\kappa^2)/(2k)}^{2k} \frac{[q^2 + (1 + \kappa^2)/3] e^{-(2/\kappa) \tan^{-1}[2\kappa/(q^2 - \kappa^2 + 1)]} dq}{[(q + \kappa)^2 + 1]^3 [(q - \kappa)^2 + 1]^3 q}. \quad (\text{A2})$$

The distribution of secondary electrons is given by

$$S_0(\kappa, k_T) = C \int_{\sqrt{\kappa^2 + 1}}^{\infty} e^{-k^2/k_T^2} \frac{d\sigma}{d\kappa} 4\pi k^3 dk, \quad (\text{A3})$$

where $k_T^2 = E_T$ is the energy of the thermal electrons normalized to the Rydberg energy. Figure 2 shows S_0/C as function of κ for different normalized energies E_T , and shows that most of the emitted electrons have energies comparable to the ionization energy.

¹P. Helander and P. J. Catto, Phys. Plasmas **8**, 1988 (2001).

²T. M. Antonsen and K. R. Chu, Phys. Fluids **25**, 1295 (1982).

³F. L. Hinton, R. E. Waltz, and J. Candy, Phys. Plasmas **11**, 2433 (2004).

⁴F. L. Hinton and R. D. Hazeltine, Rev. Mod. Phys. **48**, 239 (1976).

⁵P. Helander and D. J. Sigmar, *Collisional Transport in Magnetized Plasmas* (Cambridge University Press, Cambridge, 2002).

⁶Y. R. Lin-Liu and F. L. Hinton, Phys. Plasmas **4**, 4179 (1997).

⁷M. N. Rosenbluth, R. D. Hazeltine, and F. L. Hinton, Phys. Fluids **15**, 116 (1972).

⁸S. P. Hirshman and D. J. Sigmar, Nucl. Fusion **21**, 1079 (1981).

⁹L. Spitzer and R. Härm, Phys. Rev. **89**, 977 (1953).

¹⁰S. I. Braginskii, in *Reviews of Plasma Physics*, edited by M. A. Leontovich (Consultants Bureau, New York, 1965), Vol. 1, p. 205.

¹¹A. Yu. Pigarov, S. I. Krasheninnikov, T. D. Rognlien, M. J. Schaffer, and W. P. West, Phys. Plasmas **9**, 1287 (2002).

¹²B. LaBombard, J. E. Rice, A. E. Hubbard, J. W. Hughes, M. Greenwald, J. Irby, Y. Lin, B. Lipschultz, E. S. Marmor, C. S. Pitcher, N. Smick, S. M. Wolfe, S. J. Wukitch, and the Alcator Group, Nucl. Fusion **44**, 1047 (2004).

¹³T. Ohkawa and K. H. Burrell, in *Plasma Wall Interaction, Proceedings of the International Symposium, Jülich, West Germany, 18–22 October 1976* (Pergamon, Oxford, 1977), pp. 589–598; K. H. Burrell, S. K. Wong, and T. Amano, Nucl. Fusion **20**, 1021 (1980).

¹⁴L. D. Landau and E. M. Lifshitz, *Quantum Mechanics, Course of Theoretical Physics* (Pergamon, Oxford, 1977), Vol. 3.

¹⁵N. F. Mott and H. S. W. Massey, *The Theory of Atomic Collisions* (Oxford University Press, 1987), Vol. 2, p. 490, Eq. (99).

¹⁶K. Omidvar, Phys. Rev. **177**, 212 (1969).